Monitoring functional RNA binding of RNA-dependent ATPase enzymes such as SF2 helicases using RNA dependent ATPase assays: A RIG-I case study

Rong Guo[1] and Anna Marie Pyle[2, 3,*]

[1] Department of Chemistry

[2] Department of Molecular, Cellular, and Developmental Biology

[3] Howard Hughes Medical Institute

Yale University; New Haven, Connecticut 06520

*To whom correspondence may be addressed.

E-mail: anna.pyle@yale.edu

Mailing address:
266 Whitney Avenue
YSB 306
New Haven, CT 06520
(203) 432 - 5633

Contents

Abstract

The highly conserved Superfamily 1 (SF1) and Superfamily 2 (SF2) nucleic acid-dependent ATPases, are ubiquitous motor proteins with central roles in DNA and RNA metabolism (Jankowsky & Fairman, 2007). These enzymes require RNA or DNA binding to stimulate ATPase activity, and the conformational changes that result from this coupled behavior are linked to a multitude of processes that range from nucleic acid unwinding to the flipping of macromolecular switches (Pyle, 2008, 2011). Knowledge about the relative affinity of nucleic acid ligands is crucial for deducing mechanism and understanding biological function of these enzymes. Because enzymatic ATPase activity is directly coupled to RNA binding in these proteins, one can utilize their ATPase activity as a simple reporter system for monitoring functional binding of RNA or DNA to an SF1 or SF2 enzyme. In this way, one can rapidly assess the relative impact of mutations in the protein or the nucleic acid and obtain parameters that are useful for setting up more quantitative direct binding assays. Here, we describe a routine method for employing NADH-coupled enzymatic ATPase activity to obtain kinetic parameters reflecting apparent ATP and RNA binding to an SF2 helicase. First, we provide a protocol for calibrating an NADH-couple ATPase assay using the well-characterized ATPase enzyme hexokinase, which a simple ATPase enzyme that is not coupled with nucleic acid binding. We then provide a protocol for obtaining kinetic parameters (K_mATP, V_{max} and K_mRNA) for an RNA-coupled ATPase enzyme, using the double-stranded RNA binding protein RIG-I as a case-study. These approaches are designed to provide investigators with a simple, rapid method for monitoring apparent RNA association with SF2 or SF1 helicases.

1. Introduction

DNA and RNA metabolism involve the activity of numerous ATPase enzymes that require DNA or RNA binding to become activated and to undergo ATP hydrolysis (Bleichert & Baserga, 2007; Jankowsky & Fairman, 2007; Pyle, 2008; Sloan & Bohnsack, 2018). In many such cases, the ATPase active-site is not even structurally assembled or correctly aligned in the absence of RNA or DNA (Pyle, 2008, 2011). These proteins, which fall into two phylogenetically-determined superfamilies (SF1 and SF2) (Gorbalenya & Koonin, 1993), have many functions, including duplex unwinding and translocation, while some members catalyze more local changes in macromolecular structure (Jankowsky, Gross, Shuman, & Pyle, 2001; Pyle, 2008, 2011). For example, many SF2 proteins function as "smart" RNA binding proteins that use ATP binding and hydrolysis to trigger single conformational changes that lead to rearrangement of large ribonucleoprotein complexes, while others use ATPase activity to facilitate dissociation from a nucleic acid ligand structure (Dumont et al., 2006; Jankowsky et al., 2001; Pyle, 2008, 2011).

Because ATPase activity is selectively triggered by nucleic acid (NA) binding in these enzymes, one can utilize ATPase enzymatic activity as a "handle", or proxy, for monitoring NA association with the enzyme (R. K. F. Beran & Pyle, 2008; Ding, Kohlway, & Pyle, 2011). There are several advantages to this: (a). DNA or RNA-dependent ATPase activity reflects *functional binding* of NA to the protein, which can therefore be distinguished from nonspecific binding that frequently occurs between NA and highly basic members of the SF1 and SF2 families. Direct binding assays cannot distinguish functional and nonspecific NA binding. (b). Because NA-dependent ATPase activity reflects functional binding, it enables the investigator to conduct structure/function studies to elucidate the ideal shape or sequence of the stimulatory NA ligand, and thereby learn about the biologically relevant NA target molecule. Alternatively, it can be used to obtain a quick readout on the effects of protein mutations. (c). NA-dependent ATPase assays are quick and simple. They do not require specialized equipment or the optimization of a direct binding assay in order to get an informative initial understanding of protein-NA affinity.

While NA-dependent ATPase assays are simple and highly informative, it is ideal to conduct them together with properly-designed direct assays of NA binding to the protein of interest. This is because NA-dependent ATPase assays do not provide a true K_d value. Rather, they provide a K_mRNA value, which should only be considered an upper limit on the estimated value of the dissociation constant, Kd. In other words, RNA or DNA binding may be much stronger (and K_d lower) than it appears from the apparent K_mRNA values obtained using this approach. This is because the sensitivity of ATPase assays depends on the amount of ATP hydrolysis that can be measured, and at very low enzyme concentrations, the total amount of ATP hydrolysis may be too small to detect using the coupled assay we describe below. Other assays, such as those using isotopically-labeled ATP, can be more sensitive and provide a K_mRNA value that is closer to the true Kd, and the reader is directed to other publications where this method is described (R. K. Beran, Lindenbach, & Pyle, 2009; R. K. Beran, Serebrov, & Pyle, 2007; Ding et al., 2011). In any of these assays, if the the actual Kd is less than (tighter than) the concentration of enzyme needed to monitor ATPase activity, then the NA-dependent activity of the enzyme will be in the stoichiometric binding regime, and cannot be considered a proxy for the actual dissociation constant, Kd. It can, however, provide useful information on relative NA binding or stoichiometry under the conditions of the assay, and it can be considered an upper bound on the

relative affinity between WT enzyme and NA ligand. For example, in the RIG-I case study provided below, RNA-dependent ATPase assays can accurately be used to monitor dsRNA binding to the enzyme if the RNA is a weak ligand (in this case, a blunt duplex with a 5'-OH terminus, Kd ~ 20 nM) (Ren, Linehan, Iwasaki, & Pyle, 2019; Vela, Fedorova, Ding, & Pyle, 2012). But it cannot be used to accurately measure binding of the highest-affinity RIG-I targets (blunt RNA duplexes terminated with a 5'-triphosphate, Kd ~ 10 pM) (Ren et al., 2019; Vela et al., 2012), which have K_d values that are several logs lower than non-phosphorylated dsRNAs.

Given its simplicity and ease of implementation, we present the following protocol for employing an enzymatically coupled ATPase assay established (De La Cruz, Sweeney, & Ostap, 2000; Imamura, Tada, & Tonomura, 1966; Lindsley, 2001; Luo et al., 2011) to monitor NA binding to a NA-dependent ATPase enzyme. To facilitate the use of this assay, we also describe the assay calibration protocol using a relatively cheap, commercially available non-nucleic acid dependent ATPase. Although we use this approach to monitor dsRNA binding by a SF2 enzyme below, one can easily adapt it to monitor NA interactions with SF1 enzymes. While the example enzyme described below (RIG-I) does not display ATPase activity in the absence of dsRNA, it is still possible to use this assay for monitoring NA binding by an enzyme with background levels of unstimulated ATPase activity (such as the NS3 enzyme from Hepatitis C Virus). In those cases, the results must simply be normalized for background hydrolysis by the enzyme(R. K. Beran et al., 2009; R. K. Beran et al., 2007; Ding et al., 2011).

2. NADH-Coupled ATPase Assay to measure RNA binding affinity

The NADH-coupled enzyme assay has been widely applied to characterize steady-state kinetics for ATPases (Beisenherz, Bucher, & Garbade, 1955; Bucher & Pfleiderer, 1955; De La Cruz et al., 2000; Imamura et al., 1966; Lindsley, 2001; Luo et al., 2011; Montpetit, Seeliger, & Weis, 2012). Instead of measuring inorganic phosphate-release, the NADH-coupled assay monitors ADP production via a multi-enzyme ATP regeneration system (Diagram 1). In this system, the ATPase of interest converts ATP into inorganic phosphate and ADP. Pyruvate kinase (PK) then converts ADP back to ATP while phosphoenolpyruvate (PEP) is transformed to pyruvate. The pyruvate is reduced to lactate by lactate dehydrogenase (LDH), which couples to the NADH oxidation reaction where NADH (which absorbs at 340 nm) is oxidized to NAD^+ (which absorbs at 260 nm). The loss in absorbance at 340 is proportional to the quantity of ATPase hydrolysis and can be monitored via spectrometric methods. In our protocol, we adapted the NADH-coupled assay to a facile, low-volume system (50 µl total volume) enabling measurement of ATPase hydrolysis rate in a conventional plate reader. Time-dependence measurements of ATP hydrolysis determines reaction velocities. In turn, ATP and RNA-concentration dependence measurements of velocity provide kinetic parameters, including the apparent binding constants or K_M values, and K_{cat} or the turnover number for the enzyme.

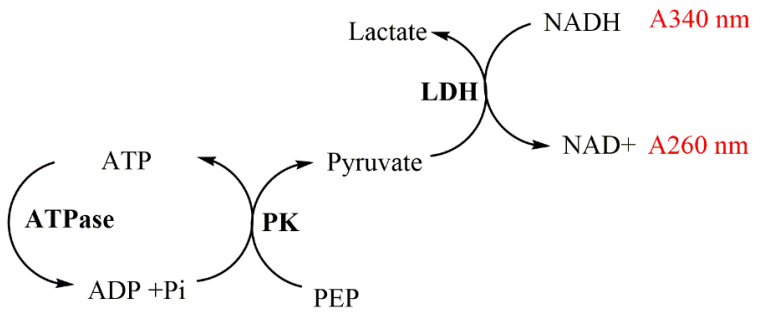

Diagram 1 . The ATPase hydrolysis reaction is coupled to the oxidation of NADH via a series of enzymatic reactions.

2.1 NADH-Coupled Reaction Preparation

To set up a 50 µl NADH-coupled reaction in a 96-well plate format, it is important to make the 5x enzyme mix containing PEP, PK, LDH and NADH (see Table 1). Then the 10 µl 5x enzyme mix is incubated with the SF2 helicase of interest, together with increasing concentrations of substrates in each well at room temperature for over one hour before the addition of ATP to initiate the reaction. The reaction details are shown below:

2.1.1. Equipment

- Plate Reader
- 96-well plates

2.1.2. Reagents and Buffers

- ATPase Assay Buffer: 25 mM HEPEs pH 7.4, 150 mM NaCl and 1.5 mM $MgCl_2$, 5 mM DTT
- NADH (Sigma N8129), powder
- Lactic dehydrogenase (LDH, Sigma L-1254), stored in 50% glycerol
- Pyruvate Kinase (PK, Sigma 1012816300), stored in 50% glycerol
- Phosphoenol pyruvic acid (PEP, Sigma, P-7127), stored in water, pH is adjusted to 7.0.

2.1.3. ATPase reaction setup and procedure

The coupled enzymes are mixed into the 5X cocktail solution showed below (Table 1). Note that the cocktail mix should be made fresh before each use. SF2 helicase and RNA will be diluted to the concentrations as needed and incubated with the 5x mix (Table 2) for at least one hour. ATP is then added to initiate the ATPase reaction. Centrifuge the plate for 3 min at 3000 rpm and start to monitor the absorbance at 340 nm over at least 15 min at 20 second intervals.

Table 1. The 5X NADH Cocktail Component

	Stock	Final Concentration
LDH	4000 U/mL	100 U/mL
PK	2000 U/mL	500 U/mL
PEP	100 mM	2.5 mM
NADH	2 mg	1 mM
ATPase Buffer	1x	

Table 2. Reaction setup (50 µl final volume)

		Stock	Desired Concentration	Volume
Incubate for at least one hour	5X cocktail mix	5x	1X	10 µl
	ATPase(SF2 helicase)	vary	2-50 nM*	vary
	Substrate (RNA)	vary	vary	vary
	ATPase Buffer	1x	1x	Add up to 45 µl
	ATP	vary	vary	5 µl

*The lowest concentration of SF2 helicase needs to be determined experimentally.

2.1.4. Data Analysis

- Obtain the slope of NADH absorbance vs time
- Convert the units from absorbance to concentration of NADH (Imamura et al., 1966) using the extinction coefficient for NADH (ε340 = 6220 $M^{-1}cm^{-1}$) via the Beer- Lambert Law (Eq.1) .

(1) $[NADH] = \frac{Abs340}{\varepsilon NADH * pathlength}$ Where ε is the extinction coefficient of NADH; pathlength of a plate is given or calculated from vendor's handbook

- The change in [NADH] vs time is equivalent to the rate of ATP hydrolysis and is in units of molarity per second.
- The ATPase hydrolysis velocity is plotted as a function of the concentration of the ligand of interest (RNA or ATP in the case of SF2 helicase). The data can be analyzed using various graphing software, such as GraphPad Prism.
- The data will be fitted to the quadratic Briggs-Haldane equation (Eq.2) and Michaelis Menten curve can be plotted and K_m and V_{max} can be extrapolated from the curve.

(2) $y = yo + (amp) \times \frac{x+p+Km-\sqrt{(x+p+Km)^2-4xp}}{2p}$

Where Y= catalytic velocity; Yo= background catalytic velocity without ATPase; amp =Vmax-Yo= Kcat; x =total substrate concentration, p= total ATPase concentration.

2.1.5. Notes

- For each ATPase reaction, a control reaction under the same conditions without ATPase and Nucleic Acid addition is needed to ensure the proper function of the assay. Low to no ATPase activity is expected for the controls.
- Plots of NADH versus time can be nonlinear, with a slope that can change at the beginning of the reaction due to the turbulence of adding ATP (red portion in Fig. 1) and it should become linear after a short period of time. Only use the linear region for determining velocity

When the NADH depleted and detection limit of the plate reader has been reached, the Abs340 nm vs time will stop changing and slope becomes flat (see blue portion of the curve, Fig. 1). Only the linear range of the Abs340 nm vs time should be used for calculation of ATPase rate.

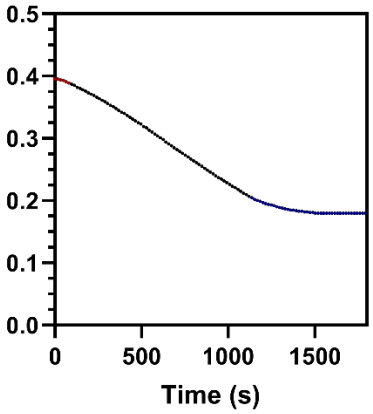

Figure 1 . Abs340 nm vs Time(s) for the NADH-coupled reaction containing RIG-I and 5' OHSLR14, initiated by 5 mM ATP. The red portion from 0 to 80 seconds represents the instability of absorbance at the beginning of the experiment. The blue portion of the curve represents the NADH is used up and plate reader is incapable of reading the changes in NADH absorbance after 16 mins.

2.2. Calibrating the ATPase Assay using Hexokinase

Due to the complexity of this multienzyme assay, it is important to validate it under local laboratory condidtions using a well-established ATPase enzyme before applying an RNA-coupled ATPase of interest. Here, we use hexokinase (HK), which is a model enzyme that converts glucose to glucose-6-phosphate with ATP hydrolysis, to calibrate the ATPase assay and we compare our kinetic parameters with values reported in the literature. It is important to note that hexokinase exists in three isozymes and the kinetic parameters of HK might vary from different sources (recombinant vs. commercially available brands). To standardize the protocol, we used the yeast hexokinase isozyme suspension from Sigma Aldrich (SKU: 11426362001). The reference values for $K_{m,\ ATP}$ and $K_{m,\ glucose}$ are 0.27 ± 0.02 mM and 0.14 ± 0.002 mM (Hillard & Stewart, 1998), which are in agreement with the past literature values (Fromm & Zewe, 1962; Gao & Leary, 2003).

2.2.1. Reaction setup

The reaction setup is based on that desccribed in section 2.1, with the following modification: ATPase buffer is changed to 50 mM MOPS pH 7.4, 1 mM $MgCl_2$ to keep consistent with the past HK kinetic studies(Hillard & Stewart, 1998).

1. 5X NADH enzyme cocktail is constituted as table 1.

To obtain Km for ATP

- Mix 0.25 U/mL (9.7 nM) HK (sigma, SKU: 11426362001) with 5 mM Glucose and 10 µL 5x NADH enzyme mix. Combine the reaction components to a total volume to 45 µL per well and centrifuge at 3000 rpm for 10 mins to ensure proper mixing. Incubate at room temperature for one hour.

- Initiate the reaction with 5 µL 10x ATP with 11 different concentrations (listed as final concentrations in reaction, µM): 0, 4.8, 9.8, 19.6, 39, 78.1, 156.3, 312.5, 625, 1250 and 2500.

To obtain Km for HK substrate: Glucose

- Mix 0.25 U/mL (9.7 nM) HK (sigma, SKU: 11426362001) with 5 uL 10x 11 different concentrations of glucose (listed as final concentrations, µM): 0, 4.8, 9.8, 19.6, 39, 78.1, 156.3, 312.5, 625, 1250 and 2500.
- Add the assay buffer and 10 µL 5x NADH enzyme mix to the total volume of 45 uL. Mix the reaction by centrifugation and incubate at room temperature for one hour
- Initiate the reaction with 5 µL 10x ATP with final concentration of 5 mM ATP.

2. Centrifuge the plate for 3 minutes at 3000 rpm and start monitor the plates at Abs340 nm for over 15 mins at 20s interval.
3. The data obtained were fitted to the quadratic Briggs-Haldane equation and analyzed as described in 2.1.4.

2.2.2. Sample data

Here, we show the Michaelis-Menten curve of ATPase rate versus ATP and Glucose (Fig. 2) obtained using the described protocol in section 2.2.1. and the analysis described in section 2.1.4. The ATPase reactions without HK show no ATPase activity (Fig. 2A). The K_mATP fitted from the curve is 0.266 ± 0.03 mM which matches well with the literature value of 0.269 ± 0.02 mM (Hillard & Stewart, 1998). Similarly, the Km, glucose is fitted to be 0.151 ± 0.02 mM which is also consistent with the reference data(Hillard & Stewart, 1998).

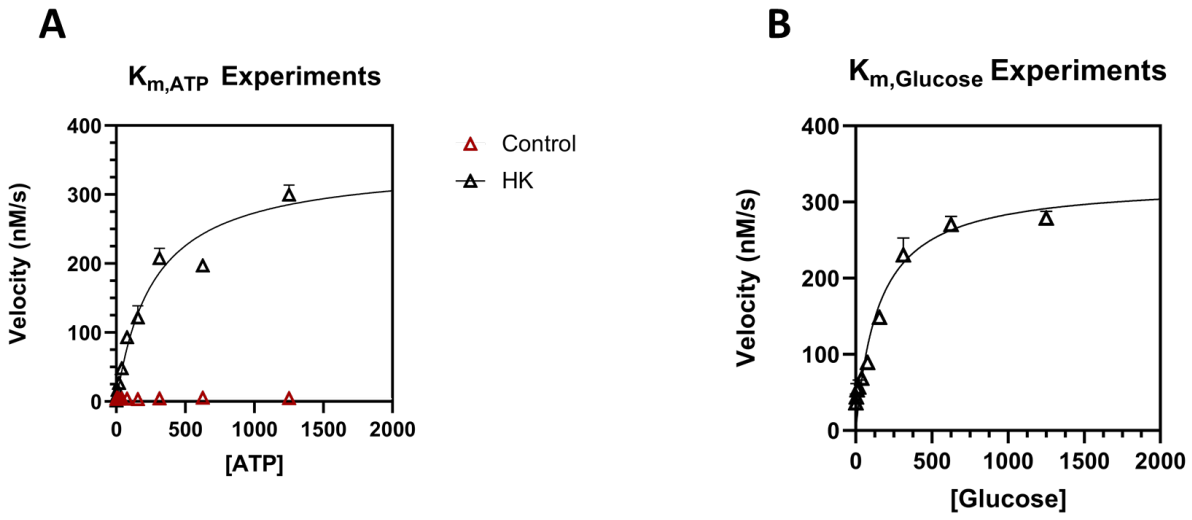

Figure 2 . Example Michaelis-Menten curve for HK. Steady state ATP hydrolysis by HK stimulated with varying concentrations of A) ATP; B) Glucose. In panel A, the control reaction without HK stimulated with different concentrations of ATP shows no catalytic activity. The extrapolated binding constant for ATP ($K_{m, ATP}$) is 0.266 ± 0.03 mM and Vmax are 346 ± 12 nM/s. $K_{m, Glucose}$ is fitted to be

0.151 ± 0.02 mM and Vmax is 326 ± 12 nM/s. Plotted values are mean ± SD (n = 3).

2.2.3. Troubleshooting Tips

The calibration of the NADH-coupled ATPase assay should provide K_m values comparable with those cited in the literature. Here are some common tips if the assay is not behaving well:

- If the NADH versus time is not linear and slope is changing, it is likely due to improper mixing or no mixing after ATP addition. Centrifuge or mixing is needed before reading the plate.
- If the slope of NADH versus time is shallow, it could be caused by 1) low concentration or loss of catalytic activity of the ATPase; 2) The pathlength of the plate is small. An Increase ATPase concentration and/or change the plate with larger pathlength to decrease signal to noise ratio.
- If the slope of NADH versus time is still shallow after increasing ATPase concentration, consider use new enzymes for constituting 5X enzyme mix.
- If the replicability of the data is not consistent, consider adding low amount of detergents such as 0.01% to 0.1 % triton to stabilize the reaction system.

2.3. Determine RNA binding affinities for SF2 protein: A RIG-I case study

Despite the diversity of SF2 enzyme biological mechanisms, all SF2 enzymes have nucleic acid dependent ATPase activity (Jankowsky & Fairman, 2007). An important topic in the field is to find the natural or optimal ligands for a given SF2 enzyme, from which the ligand recognition and activation mechanism can be further explored. To this end, a facile method that reports on the binding affinity of different nucleic acids for SF2 proteins is useful for mechanistic studies. As a case study, we use this method to determine the apparent K_m value of short, double-stranded RNA molecule binding to RIG-I, which is an important member of the SF2 family (Vela et al., 2012). Here, we measure the binding affinity between 5' OH stem-loop RNA containing 14 base pairs (5' OH SLR 14), which has been studied extensively in the past as a weak immunomodulatory ligand (Linehan et al., 2018; Ren et al., 2019)

2.3.1. Reaction setup

1. The reaction setup is described in section 2.1. In general: the 5X NADH enzyme cocktail is constituted as shown in Table 1. We will first determine the ATP saturation concentration.

To determine the Km for ATP

- Mix 50 nM WT RIG-I with 500 uM 5'OH SLR14 and 10 µL 5x NADH enzyme mix. The total mixture volume should be 45 µL per well. Centrifuge the plate at 3000 rpm for 10 mins to ensure proper mixing. Incubate at room temperature for one hour.
- Initiate the reaction with 5 µL 10x ATP with 11 different concentrations serial diluted from 2500 µM across the plate (listed as final concentrations, µM): 0, 19.6, 39, 78.1, 156.3, 312.5, 625, 1250, 2500 and 5000.

To obtain Km for 5' OH SLR14

- Mix 50 nM WT RIG-I, 10 µL 5x NADH enzyme mix and 5 uL 10x 9 different concentrations of 5'OH SLR14 across the plate (listed as final concentrations, nM): 0, 7.81, 15.63, 31.25, 62.5, 125, 250, 500 and 100.

- Add ATPase buffer to a total volume of 45 µL per well and centrifuge at 3000 rpm for 10 mins to ensure proper mixing. Incubate at room temperature for one hour.
- Initiate the reaction with 5 µL 10x ATP with final concentration of 5 mM ATP where V max is reached informed by Michaelis -Menten curve of Km,ATP (Fig. 3A)

2. Centrifuge the plate for 3 minutes at 3000 rpm and start monitor the plates at Abs340 nm for over 15 mins at 20s interval.

2.3.2. Sample Data

The ATPase data were analyzed as described in section 2.1.4 and were fitted to a Michaelis-Menten curve across ATP and RNA with increasing concentration (Fig. 3). From the ATPase rate versus ATP curve, we obtained the K_m for ATP and determined the saturation ATP concentration at 5 mM, where the velocities plateau. This high concentration of ATP is then used for stimulating ATPase activity in determining K_m for RNA experiments. The K_m for ATP is determined to be 156 ± 11 uM (Fig. 3A) and K_m for 5' OH SLR14 is 34.1 ± 5.7 nM (Fig. 3B). The obtained $K_{m,5' \text{ OH SLR14}}$ agrees with the previous directing binding data on the 14 bp blunt duplet with a 5' OH terminus where Kd is around 20 nM (Ren et al., 2019; Vela et al., 2012).

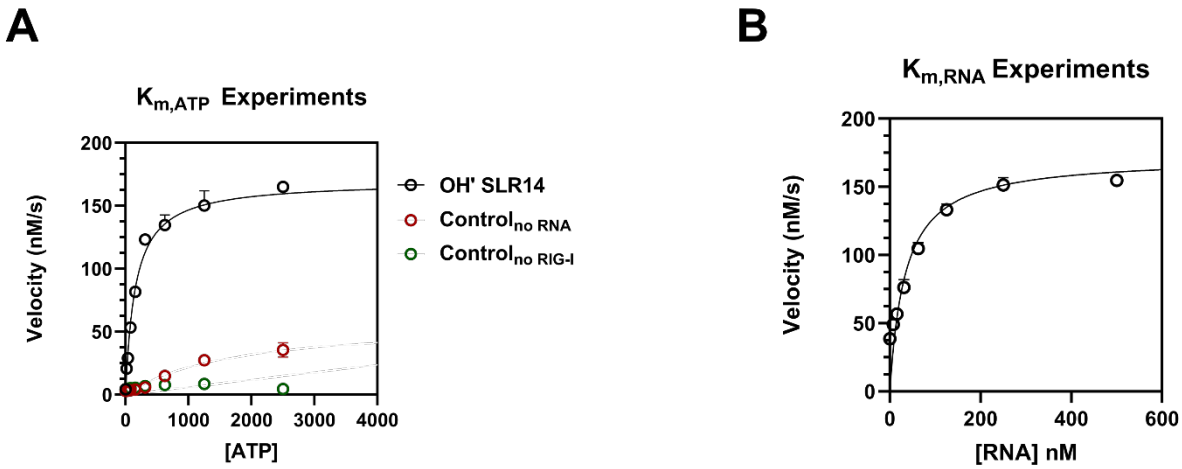

Figure 3. Michaelis-Menten curve for WT RIG-I versus ATP and RNA using 5' OH SLR14. Steady state ATP hydrolysis by wild type RIG-I proteins stimulated with varying concentrations of A) ATP; B) RNA. This experiment shows that without RIG-I or RNA, there is little detectable catalytic activity. The $K_{m,\ ATP}$ is 156 ± 11 uM and $K_{m,\ 5' \text{ OH SLR14}}$ is 34.1 ± 5.7 nM. V_{max} determined from ATP and RNA experiments is 169 ± 3.0 nM/s and is 172 ± 7.2 nM/s, respectively. Plotted values are mean ± SD (n = 3).

SUMMARY

Here, we provide a stepwise NADH-coupled assay where RNA binding affinity for RIG-I can be readily evaluated. The continuous measurement of absorbances using plate reader allows us to monitor ATP hydrolysis under various conditions simultaneously. The assay we present can serve as a model for accessing the affinity of different nucleic acid substrates for SF1 and SF2 proteins and may provide insights into their activation mechanisms.

ACKNOWLEGMENTS

AMP is an investigator of the Howard Hughes Medical Institute. RG is supported by Colton Center for Autoimmunity at Yale. We thank Dr. Dave Rawling for consultation of NADH-coupled ATPase assay and Wenshuai Wang for SF2 helicase discussion.

REFERENCES

Beisenherz, G., Bucher, T., & Garbade, K. H. (1955). Alpha-Glycerophosphate Dehydrogenase from Rabbit Muscle. *Methods in Enzymology, 1*, 391-397. doi: Doi 10.1016/0076-6879(55)01063-X

Beran, R. K., Lindenbach, B. D., & Pyle, A. M. (2009). The NS4A protein of hepatitis C virus promotes RNA-coupled ATP hydrolysis by the NS3 helicase. *J Virol, 83*(7), 3268-3275. doi: 10.1128/JVI.01849-08

Beran, R. K., Serebrov, V., & Pyle, A. M. (2007). The serine protease domain of hepatitis C viral NS3 activates RNA helicase activity by promoting the binding of RNA substrate. *J Biol Chem, 282*(48), 34913-34920. doi: 10.1074/jbc.M707165200

Beran, R. K. F., & Pyle, A. M. (2008). Hepatitis C Viral NS3-4A Protease Activity Is Enhanced by the NS3 Helicase. *Journal of Biological Chemistry, 283*(44), 29929-29937. doi: 10.1074/jbc.M804065200

Bleichert, F., & Baserga, S. J. (2007). The long unwinding road of RNA helicases. *Mol Cell, 27*(3), 339-352. doi: 10.1016/j.molcel.2007.07.014

Bucher, T., & Pfleiderer, G. (1955). Pyruvate Kinase from Muscle. *Methods in Enzymology, 1*, 435-440. doi: Doi 10.1016/0076-6879(55)01071-9

De La Cruz, E. M., Sweeney, H. L., & Ostap, E. M. (2000). ADP inhibition of myosin V ATPase activity. *Biophys J, 79*(3), 1524-1529. doi: 10.1016/S0006-3495(00)76403-4

Ding, S. C., Kohlway, A. S., & Pyle, A. M. (2011). Unmasking the Active Helicase Conformation of Nonstructural Protein 3 from Hepatitis C Virus. *Journal of Virology, 85*(9), 4343-4353. doi: 10.1128/Jvi.02130-10

Dumont, S., Cheng, W., Serebrov, V., Beran, R. K., Tinoco, I., Jr., Pyle, A. M., & Bustamante, C. (2006). RNA translocation and unwinding mechanism of HCV NS3 helicase and its coordination by ATP. *Nature, 439*(7072), 105-108. doi: 10.1038/nature04331

Fromm, H. J., & Zewe, V. (1962). Kinetic studies of yeast hexokinase. *J Biol Chem, 237*, 3027-3032.

Gao, H., & Leary, J. A. (2003). Multiplex inhibitor screening and kinetic constant determinations for yeast hexokinase using mass spectrometry based assays. *J Am Soc Mass Spectrom, 14*(3), 173-181. doi: 10.1016/S1044-0305(02)00867-X

Gorbalenya, A. E., & Koonin, E. V. (1993). Helicases - Amino-Acid-Sequence Comparisons and Structure-Function-Relationships. *Current Opinion in Structural Biology, 3*(3), 419-429. doi: Doi 10.1016/S0959-440x(05)80116-2

Hillard, S. W., & Stewart, K. K. (1998). A bypass trapped-flow analysis system evaluation of enzyme kinetic parameters with a coupled enzyme assay and fluorescence detection. *Talanta, 45*(3), 507-512. doi: 10.1016/s0039-9140(97)00180-x

Imamura, K., Tada, M., & Tonomura, Y. (1966). The pre-steady state of the myosin--adenosine triphosphate system. IV. Liberation of ADP from the myosin--ATP system and effects of modifiers on the phosphorylation of myosin. *J Biochem, 59*(3), 280-289.

Jankowsky, E., & Fairman, M. E. (2007). RNA helicases--one fold for many functions. *Curr Opin Struct Biol, 17*(3), 316-324. doi: 10.1016/j.sbi.2007.05.007

Jankowsky, E., Gross, C. H., Shuman, S., & Pyle, A. M. (2001). Active disruption of an RNA-protein interaction by a DExH/D RNA helicase. *Science, 291*(5501), 121-125. doi: 10.1126/science.291.5501.121

Lindsley, J. E. (2001). Use of a real-time, coupled assay to measure the ATPase activity of DNA topoisomerase II. *Methods Mol Biol, 95*, 57-64. doi: 10.1385/1-59259-057-8:57

Linehan, M. M., Dickey, T. H., Molinari, E. S., Fitzgerald, M. E., Potapova, O., Iwasaki, A., & Pyle, A. M. (2018). A minimal RNA ligand for potent RIG-I activation in living mice. *Sci Adv, 4*(2), e1701854. doi: 10.1126/sciadv.1701854

Luo, D., Ding, S. C., Vela, A., Kohlway, A., Lindenbach, B. D., & Pyle, A. M. (2011). Structural insights into RNA recognition by RIG-I. *Cell, 147*(2), 409-422. doi: 10.1016/j.cell.2011.09.023

Montpetit, B., Seeliger, M. A., & Weis, K. (2012). ANALYSIS OF DEAD-BOX PROTEINS IN mRNA EXPORT. *Rna Helicases, 511*, 239-254. doi: 10.1016/B978-0-12-396546-2.00011-5

Pyle, A. M. (2008). Translocation and unwinding mechanisms of RNA and DNA helicases. *Annu Rev Biophys, 37*, 317-336. doi: 10.1146/annurev.biophys.37.032807.125908

Pyle, A. M. (2011). RNA helicases and remodeling proteins. *Curr Opin Chem Biol, 15*(5), 636-642. doi: 10.1016/j.cbpa.2011.07.019

Ren, X., Linehan, M. M., Iwasaki, A., & Pyle, A. M. (2019). RIG-I Selectively Discriminates against 5'-Monophosphate RNA. *Cell Rep, 26*(8), 2019-2027 e2014. doi: 10.1016/j.celrep.2019.01.107

Sloan, K. E., & Bohnsack, M. T. (2018). Unravelling the Mechanisms of RNA Helicase Regulation. *Trends Biochem Sci, 43*(4), 237-250. doi: 10.1016/j.tibs.2018.02.001

Vela, A., Fedorova, O., Ding, S. C., & Pyle, A. M. (2012). The thermodynamic basis for viral RNA detection by the RIG-I innate immune sensor. *J Biol Chem, 287*(51), 42564-42573. doi: 10.1074/jbc.M112.385146